National Conference with International Participation
ENGINEERING MECHANICS 2007
Svratka, Czech Republic, May 14 – 17, 2007

MODELLING OF THE RAILWAY WHEELSET MOVEMENT CONSIDERING REAL GEOMETRY

R. Jandora[1]

Summary: *Problem of wheelset rolling on rails is commonly solved problem of engineering practice. Only ideal geometry of the wheelset is used in majority of studies to simulate its movement. However, shape irregularities appear as a result of wear and they have great influence on the movement. In this paper a model is presented which can be used to simulate wheelset motion in the three dimensional space. Shape irregularities are implemented into the model and diverse ways to calculate the contact forces are presented and compared with respect to accuracy of results they provide and their demands on computer equipment.*

1. Introduction

Problem of wheelset rolling on rails is commonly solved problem of engineering practice. The goal of plenty of studies published on this theme is to achieve minimisation of wear of both wheels and rails. Other studies investigate problem of vibration and noise brought on railway vehicles by corrugation of wheels and rails.

Most common models used for studying three dimensional movements of wheelsets as presented in (Dukkipati, 2000; Iwnicki, 2006; Svigler & Vimmr, 2006) do not consider influence of corrugation, only ideal geometry is used. However, shape irregularities appear as a result of wear and they have great influence on the wheelset movement. Other studies (as K. Knothe's contribution to (Jacobson & Kalker, 2000) use only two-dimensional models for modelling of corrugation on rails or out-of-round wheels.

However, both real wheelset motion and shape irregularities of wheels and rails have great influence on railway vehicle dynamics. In this paper a model is presented which can be used to simulate wheelset movement in the three dimensional space. Shape irregularities are implemented into the model and diverse ways to calculate the contact forces are presented.

2. Coordinate systems

Main coordinate system is connected to the rails. The x-axis is tangential to the centreline of the rails, the y-axis lies in direction of placing of the sleepers and the z-axis is normal to the plane of rails. Another coordinate system is connected to the wheelset. This one can have Cartesian or cylindrical representation and both use the same y_d-axis which is oriented along the wheelset axis. The other two axes (x_d, z_d) are normal to the y_d-axis and can be represented in cylindrical dimensions R_d and α_d.

[1] Ing. Radek Jandora, Ústav mechaniky těles, mechatroniky a biomechaniky, Fakulta strojního inženýrství, Vysoké učení technické v Brně; Technická 2, 616 69 Brno; tel. +420-541142804; e-mail: radek.jandora@seznam.cz

Relation between the main coordinate system and the wheelset coordinate system is described with use of three angles (see fig. 1):

ψ – angle between the wheelset axis projection into the ground plan and the main y-axis,

ϑ – angle between the wheelset axis and the horizontal plane,

φ – immediate value of the wheelset rotation.

These angles are similar to Euler angles so they determine the transformation matrix from the wheelset coordinate system into the main coordinate system.

$$\mathbf{C}_D = \mathbf{C}_D(\psi, \vartheta, \varphi) \tag{1}$$

The wheelset is moving so the matrix of angular velocity $\mathbf{\Omega}_D$ is defined:

$$\boldsymbol{\omega}_D = \begin{bmatrix} \omega_x \\ \omega_y \\ \omega_z \end{bmatrix} = \begin{bmatrix} \dot{\vartheta} \cdot \cos\psi + \dot{\varphi} \cdot \sin\psi \cdot \cos\vartheta \\ \dot{\vartheta} \cdot \sin\psi - \dot{\varphi} \cdot \cos\psi \cdot \cos\vartheta \\ \dot{\psi} - \dot{\varphi} \cdot \sin\vartheta \end{bmatrix} \rightarrow \mathbf{\Omega}_D \tag{2}$$

Position and velocity of the centre of gravity of the wheelset is

$$\mathbf{x}_t = \begin{bmatrix} x_t & y_t & z_t \end{bmatrix}^T \tag{3}$$

$$\dot{\mathbf{x}}_t = \begin{bmatrix} \dot{x}_t & \dot{y}_t & \dot{z}_t \end{bmatrix}^T \tag{4}$$

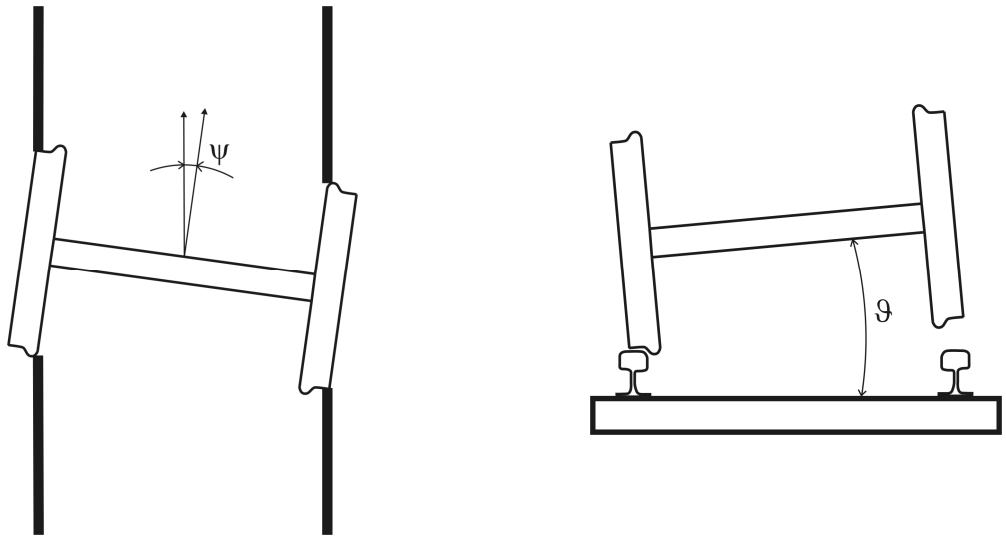

a) Top view b) Front view

Fig. 1. Position of the wheelset in the main coordinate system

3. Wheel-rail contact

Contact of each wheel-rail pair on the left side or on the right side is solved separately. Each one has its geometry described with its own functions and contact forces are calculated for either pair. However, the algorithm is same for both sides so it is not presented separately. But it has to be expressed, that the following calculations have to be followed through for both left and right wheel-rail contact pair.

3.1. Geometry

Shape of the wheel is described with the function R (fig. 2) which is the sum of the ideal wheel shape R_{id} and the shape irregularities R_{irr}:

$$R(\alpha_d, y_d) = R_{id}(y_d) + R_{irr}(\alpha_d, y_d) \tag{5}$$

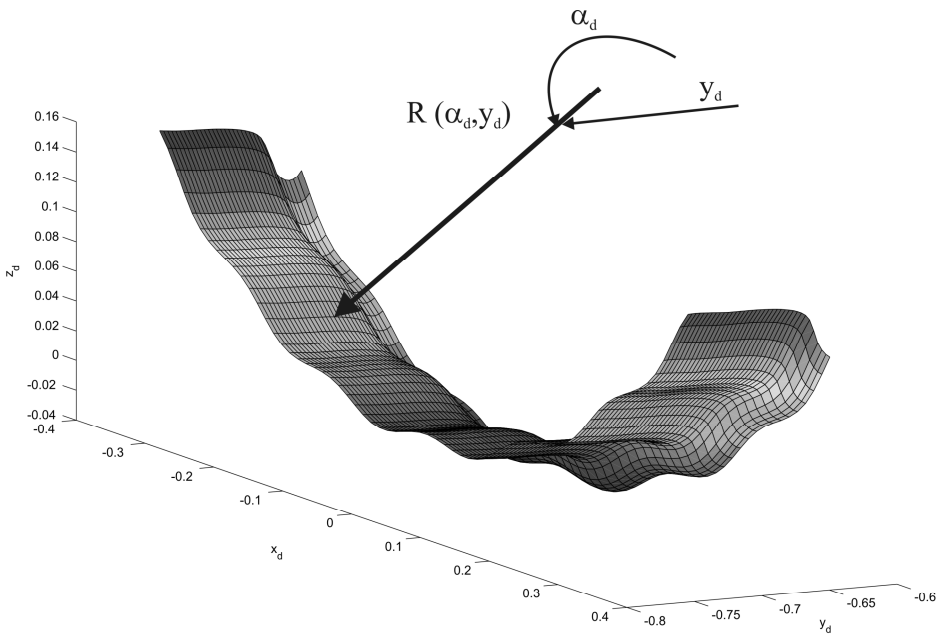

Fig. 2. Example of the wheel with shape irregularities

Function of the rail surface N (fig. 3) is sum of the actual deflection of the rail $N_{d,t}$, the ideal shape of the rail N_{id} (including placement of the rail under the 1:20 or 1:40 angle) and the corrugation N_{irr}

$$N(x,y) = N_{d,t}(x) + N_{id}(x,y) + N_{irr}(x,y) \tag{6}$$

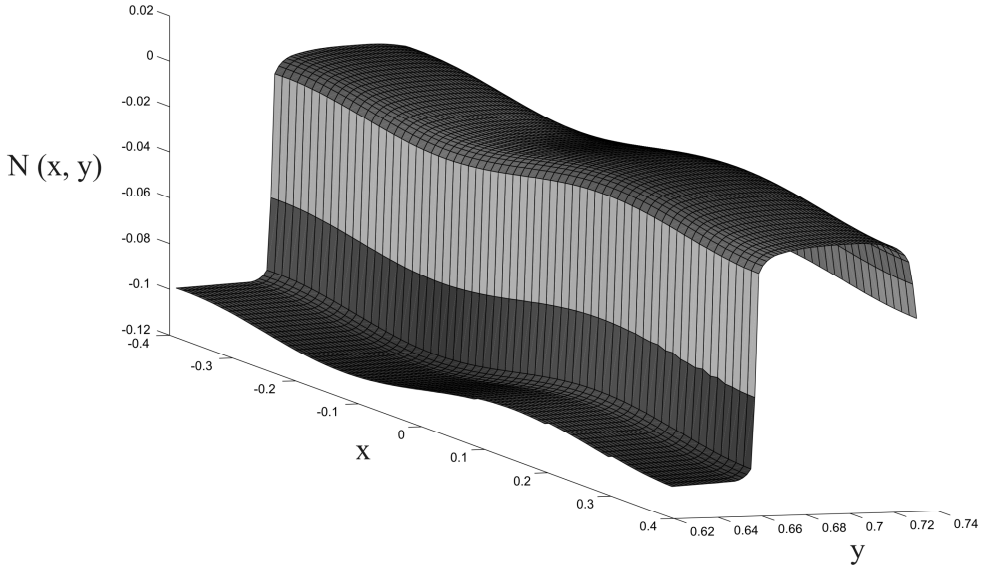

Fig. 3. Example of the rail with corrugation

Function of distance between the wheel and the rail $h = h(\alpha_d, y_d)$ is fundamental for solving the contact forces. Point of the wheel surface in the wheelset Cartesian coordinate system is

$$\mathbf{x}_d = \left[R \cdot \cos\alpha_d \quad y_d \quad R \cdot \sin\alpha_d \right]^T \tag{7}$$

In the main coordinate system it is

$$\mathbf{x}_w = \mathbf{C}_D \cdot \mathbf{x}_d + \mathbf{x}_L \tag{8}$$

The normal to the surface is found as

$$\begin{aligned}
\mathbf{t}_{w1} &= \left[\frac{dR}{d\alpha_d} \cdot \cos\alpha_d - R \cdot \sin\alpha_d \quad 0 \quad \frac{dR}{d\alpha_d} \cdot \sin\alpha_d + R \cdot \cos\alpha_d \right]^T \\
\mathbf{t}_{w2} &= \left[\frac{dR}{dy_d} \cdot \cos\alpha_d \quad 1 \quad \frac{dR}{dy_d} \cdot \sin\alpha_d \right]^T \\
\mathbf{n}_w &= \frac{\mathbf{t}_{w1} \times \mathbf{t}_{w2}}{\left\| \mathbf{t}_{w1} \times \mathbf{t}_{w2} \right\|} \\
\mathbf{n}_w &= \left[n_{w,x} \quad n_{w,y} \quad n_{w,z} \right]^T_{kart} \rightarrow \left[n_{w,\rho} \quad n_{w,\varphi} \quad n_{w,\vartheta} \right]^T_{sfer}
\end{aligned} \tag{9}$$

Point of the rail surface is defined as

$$\begin{aligned}
x_r &= \left[x_{r,1} \quad x_{r,2} \quad x_{r,3} \right]^T \\
x_{r,1} &= -h \cdot \cos\left(n_{w,\varphi}\right) \cdot \sin\left(n_{w,\vartheta}\right) + x_{w,1} \\
x_{r,2} &= -h \cdot \sin\left(n_{w,\varphi}\right) \cdot \sin\left(n_{w,\vartheta}\right) + x_{w,2} \\
x_{r,3} &= N\left(x_{r,1}, x_{r,2}\right)
\end{aligned} \tag{10}$$

These equations mean that the point of interest lies on the normal of the wheel surface in unknown distance *h*. This distance is found by solving the nonlinear equation

$$0 = -h \cdot \cos\left(n_{w,\vartheta}\right) + x_{w,3} - x_{r,3}\left(h\right) \tag{11}$$

Thus the distance $h\left(\alpha_d, y_d\right)$ for every point of the wheel surface can be found.

3.2. Contact forces

When solving the contact forces in the wheel rail contact, two different approaches can be used. It can be assumed that the contact patch is in the shape of ellipse or that the contact patch has a general shape.

A) Hertzian contact

Hertz theory of contact (Hertz, 1881) assumes that the contact patch is elliptic. Minimum of the distance function $h\left(\alpha_d, y_d\right)$ can be found with the simplex method. It can be greater than zero (then there is a gap between the wheel and the rail) or less than zero (then the wheel and the rail are in contact and deformed). In the extreme the centre of the contact ellipse is expected. In order to find the contact forces three steps have to be completed – principal coordinate system and principal curvatures of the contact patch have to be found and then normal and tangential forces have to be calculated.

1) Principal coordinate system and principal curvatures of the contact patch

Algorithm of finding principal coordinate system and principal curvatures of surface is described in (Budinsky, 1983). Points of the surface $\mathbf{x}_s$ are functions of two parameters u_1 and u_2

$$\mathbf{x}_s = \left[x_{s,1}\left(u_1, u_2\right) \quad x_{s,2}\left(u_1, u_2\right) \quad x_{s,3}\left(u_1, u_2\right) \right]^T \tag{12}$$

Tangential vectors of the surface are

$$t_{j,i} = \frac{\partial x_{s,i}}{\partial u_j} \qquad i = 1,\ 2,\ 3;\ j = 1,\ 2 \tag{13}$$

Normal vector of the surface is

$$\mathbf{n} = \frac{\mathbf{t}_1 \times \mathbf{t}_2}{\left\| \mathbf{t}_1 \times \mathbf{t}_2 \right\|} \tag{14}$$

Matrix **G** of the first fundamental form of the surface is

$$G_{ij} = \mathbf{t}_i \cdot \mathbf{t}_j \qquad i = 1,\ 2;\ j = 1,\ 2 \tag{15}$$

Matrix **H** of the second fundamental form of the surface is

$$H_{ij} = \mathbf{n} \cdot \frac{\partial^2 \mathbf{x}_s}{\partial u_i\, \partial u_j} \qquad i = 1,\ 2;\ j = 1,\ 2 \tag{16}$$

Principal curvatures C_v of the surface are eigenvalues of the matrix $\mathbf{H} \cdot \mathbf{G}^{-1}$ and they can be solved using equation

$$\left(\mathbf{H} \cdot \mathbf{G}^{-1} - C_v \cdot \mathbf{I} \right) \cdot \mathbf{w} = 0 \tag{17}$$

Outputs of the eigenvalue algorithm are matrices $\mathbf{C}_v$ (eigenvalues) and **W** (eigenvectors)

$$\mathbf{C}_v = \begin{bmatrix} C_{v,1} & 0 \\ 0 & C_{v,2} \end{bmatrix} \tag{18}$$

$$\mathbf{W} = \begin{bmatrix} w_{1,1} & w_{1,2} \\ w_{2,1} & w_{2,2} \end{bmatrix} \tag{19}$$

Using the eigenvectors and tangential vectors of the surface two principal directions of the surface are found

$$\mathbf{t}_{p,i} = \frac{w_{j,i} \cdot \mathbf{t}_j}{\left\| w_{j,i} \cdot \mathbf{t}_j \right\|} \qquad i = 1,\ 2;\ j = 1,\ 2 \tag{20}$$

Principal coordinate system of the surface is created from properly arranged principal vectors of the surface and the normal of the surface

$$\mathbf{C}_{PS} = \begin{bmatrix} \mathbf{t}_{p,1} & \mathbf{t}_{p,2} & \mathbf{n} \end{bmatrix} \tag{21}$$

Function of the surface of the wheel (in the wheelset coordinate system) is

$$\mathbf{x}_d = \begin{bmatrix} R(\alpha_d, y_d) \cdot \cos\alpha_d & y_d & R(\alpha_d, y_d) \cdot \sin\alpha_d \end{bmatrix}^T \tag{22}$$

where α_d and y_d are the parameters of the surface. Function of the surface of the rail (in the main coordinate system) is

$$x_r = \begin{bmatrix} x & y & N(x, y) \end{bmatrix} \tag{23}$$

where x and y are the parameters of the surface. By following the presented algorithm principal coordinate system of the wheel $\mathbf{C}_{PS,W}$ and principal coordinate system of the rail $\mathbf{C}_{PS,R}$ is obtained.

Undeformed distance of surfaces is generally

$$h = \frac{1}{2}(A_1 + A_2)x_1^2 + (C_1 + C_2)x_1 x_2 + \frac{1}{2}(B_1 + B_2)x_2^2 \tag{24}$$

However, the middle term $(C_1 + C_2)x_1 x_2$ has zero value in the Hertz theory of contact. Therefore both principal coordinate system of the wheel and principal coordinate system of the rail have to be rotated into the common principal coordinate system where the term $(C_1 + C_2)x_1 x_2$ vanishes (Kalker, 1990).

Both surfaces have common normal and they are rotated against each other by angle ε. The angle by which coordinate system of the wheel has to rotate into the common principal coordinate system is

$$\varepsilon_w = \frac{1}{2} \cdot \arctan\left(\frac{\sin 2\varepsilon}{\cos 2\varepsilon - \frac{C_{w,1} - C_{w,2}}{C_{r,1} - C_{r,2}}} \right) \tag{25}$$

and the angle of rotation from principal coordinate system of the rail into the common principal coordinate system is

$$\varepsilon_r = \varepsilon_w - \varepsilon \tag{26}$$

Thus the transformation matrices are

$$\mathbf{T}_w = \begin{bmatrix} \cos\omega_w & -\sin\omega_w & 0 \\ \sin\omega_w & \cos\omega_w & 0 \\ 0 & 0 & 1 \end{bmatrix} \tag{27}$$

$$\mathbf{T}_r = \begin{bmatrix} \cos\omega_r & -\sin\omega_r & 0 \\ \sin\omega_r & \cos\omega_r & 0 \\ 0 & 0 & 1 \end{bmatrix} \tag{28}$$

$$\mathbf{T}_{w2} = \begin{bmatrix} \cos\omega_w & -\sin\omega_w \\ \sin\omega_w & \cos\omega_w \end{bmatrix} \tag{29}$$

$$\mathbf{T}_{r2} = \begin{bmatrix} \cos\omega_r & -\sin\omega_r \\ \sin\omega_r & \cos\omega_r \end{bmatrix} \tag{30}$$

The common principal coordinate system is then

$$\mathbf{C}_{PS} = \mathbf{C}_{PS,w} \cdot \mathbf{T}_w = \mathbf{C}_{PS,r} \cdot \mathbf{T}_r \tag{31}$$

2) Hertzian normal force

Undeformed distance of the surfaces in contact according to the Hertz theory of contact as presented in (Johnson, 1985; Kalker, 1990; Jacobson & Kalker, 2000) is in the form of

$$h = D_{1,1} x_1^2 + D_{2,2} x_2^2 - q \tag{32}$$

Constants $D_{1,1}$ and $D_{2,2}$ are common principal curvatures acquired from

$$\mathbf{D} = \frac{1}{2} \cdot \left(\mathbf{T}_{w2} \cdot \mathbf{C}_w \cdot \mathbf{T}_{w2}^T - \mathbf{T}_{r2} \cdot \mathbf{C}_r \cdot \mathbf{T}_{r2}^T \right) \tag{33}$$

and they are used to get angle t_{ax} from

$$\cos t_{ax} = \left| \frac{D_{1,1} - D_{2,2}}{D_{1,1} + D_{2,2}} \right|$$

The value $\cos t_{ax}$ is input into the axial function

$$\cos t_{ax} = m^2 \frac{\mathbf{D}\left(m^2\right) - \mathbf{C}\left(m^2\right)}{\mathbf{E}\left(m^2\right)} \tag{34}$$

where functions **C**, **D** and **E** are complete elliptic integrals (see Kalker, 1990). From the axial function excentricity m of the contact ellipse is acquired. Then, according to the common principal curvatures $D_{1,1}$ and $D_{2,2}$, ratio of squares of the half-axes of the contact ellipse is found

$$k_e = \frac{b_{ce}^2}{a_{ce}^2}$$

$$k_e = \begin{cases} 1-m^2 & \text{for} \quad D_{1,1} \le D_{2,2} \\ \dfrac{1}{1-m^2} & \text{for} \quad D_{1,1} > D_{2,2} \end{cases} \tag{35}$$

Another elliptic integrals, **K** and **E** are required:

$$\mathbf{K} = EllipticK\left(m^2\right)$$

$$\mathbf{E} = EllipticE\left(m^2\right)$$

The normal force is then

$$N = \frac{2\pi G}{3(1-\mu)} \cdot \sqrt{\frac{\mathbf{E}(-h)^3}{\left(D_{1,1}+D_{2,2}\right)k_e \mathbf{K}^3}} \tag{36}$$

and half-axes of the contact ellipse are

$$a_{ce} = \sqrt[3]{\frac{3N(1-\mu)\mathbf{E}}{2\pi G\left(D_{1,1}+D_{2,2}\right)k_e}} \tag{37}$$

$$b_{ce} = a_{ce}\sqrt{k_e} \tag{38}$$

G is the modulus of rigidity and μ is the Poisson's ratio.

3) Tangential forces

Tangential forces in the contact ellipse can be solved in different ways. Three of them are described below. Each of them requires the rolling velocity to be known. The x-component of the wheelset velocity can be considered the rolling velocity:

$$\mathbf{v}_{rol} = \begin{bmatrix} \dot{x}_t & 0 & 0 \end{bmatrix}^T \tag{39}$$

The contact patch has different orientation than the main coordinate system so projection into the plane of the contact patch is needed

$$\mathbf{v}_{rol,r} = \begin{bmatrix} 1 & 0 & 0 \\ 0 & 1 & 0 \\ 0 & 0 & 0 \end{bmatrix} \cdot \mathbf{C}_{PS}^T \cdot \mathbf{v}_{rol} \tag{40}$$

Magnitude of the rolling velocity is

$$V = \left\| \mathbf{v}_{rol,r} \right\| \tag{41}$$

Rolling contact theories assume the x-axis of the contact patch is identical with the direction of the rolling velocity; therefore the common principal coordinate system of the contact patch has to be once again rotated by the angle ε_{rol}

$$\varepsilon_{rol} = \arctan \frac{v_{rol,r,y}}{v_{rol,r,x}} \tag{42}$$

$$\mathbf{T}_{rol} = \begin{bmatrix} \cos\varepsilon_{rol} & -\sin\varepsilon_{rol} & 0 \\ \sin\varepsilon_{rol} & \cos\varepsilon_{rol} & 0 \\ 0 & 0 & 1 \end{bmatrix} \tag{43}$$

Velocity of the point of the wheel which is the centre of the contact ellipse is

$$\dot{\mathbf{x}}_w = \mathbf{\Omega}_D \cdot \mathbf{C}_D \cdot \mathbf{x}_d + \dot{\mathbf{x}}_t \tag{44}$$

Angular velocity of the wheelset is $\boldsymbol{\omega}_D$ (from eq. 2). In order to calculate the contact forces they have to be transformed into the coordinate system of the projection of the rolling velocity:

$$\dot{\mathbf{x}}_{w,r} = \mathbf{T}_{rol}^T \cdot \mathbf{C}_{PS}^T \cdot \dot{\mathbf{x}}_w \tag{45}$$

$$\boldsymbol{\omega}_{L,r} = \mathbf{C}_{PS}^T \cdot \boldsymbol{\omega}_D \tag{46}$$

The rail is not moving so these values are the rigid slip and the rigid spin in the contact patch. Values of the longitudinal creepage υ_x, lateral creepage υ_y and spin creepage φ_z are

$$\upsilon_x = \frac{x_{w,r,1}}{V} \tag{47}$$

$$\upsilon_y = \frac{x_{w,r,2}}{V} \tag{48}$$

$$\varphi_z = \frac{\omega_{D,r,3}}{V} \tag{49}$$

Now the contact forces can be calculated.

a) Linear theory of rolling contact

The linear theory of rolling contact (Kalker, 1990) assumes adhesion in the whole contact patch. The tangential forces and the spin moment have linear dependence on the creepages

$$T_x = -GabC_{11}\upsilon_x \tag{50}$$

$$T_y = -GabC_{22}\upsilon_y - G(ab)^{\frac{3}{2}} C_{23}\varphi_z \tag{51}$$

$$M_z = -G(ab)^{\frac{3}{2}} C_{32}\upsilon_y - G(ab)^2 C_{33}\varphi_z \tag{52}$$

Here C_{11}, C_{22}, $C_{23} = -C_{32}$ and C_{33} are Kalker's creepage coefficients which are calculated numerically and tabulated (in Kalker, 1990; Johnson, 1985).

b) Vermeulen & Johnson theory

While the contact forces are linearly dependent on creepages in the previous step, in reality they saturate on value

$$T = fN \tag{53}$$

Therefore accordingly to the Vermeulen & Johnson theory as presented in (Kalker, 1990) the tangential forces calculated by the linear theory are modified by the following algorithm:

$$T = \sqrt{T_x^2 + T_y^2} \tag{54}$$

$$w' = \frac{T}{3fN} \tag{55}$$

$$\overline{T} = \begin{cases} fN\left[1-(1-w')^2\right] & \text{pro} \quad w' \le 1 \\ fN & \text{pro} \quad w' > 1 \end{cases} \tag{56}$$

$$\overline{T}_x = \frac{T_x}{T}\overline{T} \tag{57}$$

$$\overline{T}_y = \frac{T_y}{T}\overline{T} \tag{58}$$

Now slip is taken into account. However, the Vermeulen and Johnson theory is applicable only when spin is zero or insignificant.

c) FASTSIM algorithm

The FASTSIM algorithm (Kalker, 1990; Jacobson & Kalker, 2000) has to be applied in order to calculate the contact forces when spin is significant. Then the contact area is discretized and the simplified theory of contact is used. This way the solution is slower, however not only more accurate force estimation is acquired but also approximate pressure and slip distribution is calculated. Only restrictions of the FASTSIM algorithm are that it can be used only for quasiidentical bodies (bodies made of the same or similar material) and for elliptical contacts (Kalker's creepage coefficients are required).

B) Non-Herzian contact

When more accurate solution is demanded, other methods have to be used. The contact patch of the wheel-rail contact is often non-Hertzian (non-elliptical). Then numerical methods of estimation of both normal and tangential traction need to be applied.

a) CONTACT algorithm

The CONTACT algorithm created by Kalker (described in Kalker, 1990; Jacobson & Kalker, 2000) is a method based on boundary element method and methods of nonlinear optimization. The expected contact area is divided into elements and the representation of Boussinesq and Cerruti (Johnson, 1985; Kalker, 1990) is integrated over each element. In two stages (NORM and TANG) the normal and tangential tractions are calculated.

Building of the influence number matrices and multiple building and solving of system of equations in both NORM and TANG algorithms is very slow and memory-consuming process relative to the analytical solutions or the FASTSIM algorithm. However, the wheel-rail contact is often non-Hertzian, especially when the flange touches the edge of the rail. Advantage of the CONTACT algorithm is that more accurate pressure and slip distributions are obtained.

b) FEA

Finite element analysis is universal method to calculate forces in the wheel-rail contact. A great advantage is that shape of the whole wheel can be taken into account and even stresses inside the bodies are found. However, the finite element analysis is also the most time- and memory-consuming method.

3.3. Equations of motion and state function

Contact forces calculated by any method are placed in the coordinate system of the projection of the rolling velocity. In order to build equations of motion they have to be transformed into the main coordinate system:

$$\mathbf{F}_{con,r} = \begin{bmatrix} \bar{T}_x & \bar{T}_y & N \end{bmatrix}^T \tag{59}$$

$$\mathbf{M}_{con,r} = \begin{bmatrix} 0 & 0 & M_z \end{bmatrix}^T \tag{60}$$

$$\mathbf{F}_{con} = \mathbf{C}_{SP} \cdot \mathbf{T}_{rol} \cdot \mathbf{F}_{con,r} \tag{61}$$

$$\mathbf{M}_{con} = \mathbf{C}_{SP} \cdot \mathbf{M}_{con,r} \tag{62}$$

All exterior forces and moments affecting the wheelset from connected bodies (springs, dampers, resistance) are summed into force

$$\mathbf{F}_e = \begin{bmatrix} F_{e,x} & F_{e,y} & F_{e,z} \end{bmatrix}^T \tag{63}$$

and moment

$$\mathbf{M}_e = \begin{bmatrix} M_{e,x} & M_{e,y} & M_{e,z} \end{bmatrix}^T \tag{64}$$

Position of the contact patch relative to the centre of gravity of the wheelset is

$$\begin{aligned} \mathbf{r}_{con} &= \mathbf{x}_w - \mathbf{x}_t = \mathbf{C}_D \cdot \mathbf{x}_d + \mathbf{x}_t - \mathbf{x}_t \\ \mathbf{r}_{con} &= \mathbf{C}_D \cdot \mathbf{x}_d \end{aligned} \tag{65}$$

The equations of motion of the wheelset are

$$\ddot{\mathbf{x}}_t = \frac{1}{m} \cdot \left(\mathbf{F}_{con}^L + \mathbf{F}_{con}^R + \mathbf{F}_v \right) + \mathbf{g} \tag{66}$$

$$\boldsymbol{\alpha} = \mathbf{J}^{-1} \cdot \left(\mathbf{r}_{con}^L \times \mathbf{F}_{con}^L + \mathbf{r}_{con}^R \times \mathbf{F}_{con}^R + \mathbf{M}_{con}^L + \mathbf{M}_{con}^R + \mathbf{M}_v \right) \tag{67}$$

The vector of angular acceleration $\boldsymbol{\alpha}$ is transformed to $\ddot{\psi}$, $\ddot{\vartheta}$ a $\ddot{\varphi}$:

$$\ddot{\psi} = \frac{\alpha_x \cdot \sin\psi \cdot \sin\vartheta - \alpha_y \cdot \cos\psi \cdot \sin\vartheta + \alpha_z \cdot \cos\vartheta + \dot{\psi} \cdot \dot{\vartheta} \cdot \sin\vartheta + \dot{\vartheta} \cdot \dot{\varphi}}{\cos\vartheta} \tag{68}$$

$$\ddot{\varphi} = \frac{a_x \cdot \sin\psi - \alpha_y \cdot \cos\psi + \dot{\psi} \cdot \dot{\vartheta} + \dot{\vartheta} \cdot \dot{\varphi} \cdot \sin\vartheta}{\cos\vartheta} \tag{69}$$

$$\ddot{\vartheta} = \alpha_x \cdot \cos\psi + \alpha_y \cdot \sin\psi - \dot{\psi} \cdot \dot{\varphi} \cdot \cos\vartheta \tag{70}$$

Thus the state function

$$\left[\dot{x}_t,\, \ddot{x}_t,\, \dot{y}_t,\, \ddot{y}_t,\, \dot{z}_t,\, \ddot{z}_t,\, \dot{\psi},\, \ddot{\psi},\, \dot{\vartheta},\, \ddot{\vartheta},\, \dot{\varphi},\, \ddot{\varphi} \right] = f\left(\left[x_t,\, \dot{x}_t,\, y_t,\, \dot{y}_t,\, z_t,\, \dot{z}_t,\, \psi,\, \dot{\psi},\, \vartheta,\, \dot{\vartheta},\, \varphi,\, \dot{\varphi} \right] \right) \tag{71}$$

is acquired and used for numerical integration with a chosen method.

4. Conclusions

Simulation of the wheelset moving on rails with consideration of the shape irregularities requires somewhat different approach than models using ideal geometry. While in the ideal case velocities of the wheels and orientation of the contact patch coincide with the main coordinate system, in general case they can be rotated with respect to each other. Therefore all quantities describing the system have to be transformed to coincide with the geometry of the contact.

Forces in the wheel-rail contact can be calculated using a number of different methods. It appears from previous work of the author (Jandora et al., 2006) that rigid-body solutions of the wheel-rail contact are insufficient in the case of shape irregularities. So contact of elastic bodies needs to be assumed. Normal tractions can be calculated with the Hertz solution for Hertzian contacts (elliptical contact patch). Tangential tractions can be solved using the linear theory of rolling contact, the Vermeulen & Johnson theory or the FASTSIM algorithm. The linear theory does not take into account slip in the contact patch, full adhesion is expected, the Vermeulen & Johnson theory is used to calculate no spin solution of the contact forces. When spin is significant, the FASTSIM algorithm is applied. For non-Hertzian contacts which appear when the flange touches the edge of the rail, numerical methods have to be used, either the CONTACT algorithm or the finite element analysis. However, numerical solutions are very time-consuming in comparison to methods using Hertzian contact assumptions. Therefore the numerical methods should be applied only when better accuracy of the results is demanded.

5. Acknowledgement

The research has been supported by the Faculty of Mechanical Engineering of the Brno University of Technology by means of the BD1363015 grant project.

6. References

Budinsky, B. (1983): Analytical and Differential Geometry, SNTL (in Czech).

Dukkipati, R. V. (2000): Vehicle Dynamics, Narosa Publishing House.

Hertz, H. (1881): Über die Berührung fester elastischen Körper. Journal für reine und angewandte Mathematik, Bd. 92, pp. 156-171.

Iwnicki, S. (2006): Handbook of Railway Vehicle Dynamics, Taylor & Francis.

Jacobson, B., Kalker, J. J. (2000): Rolling Contact Phenomena, Springer-Verlag.

Jandora, R., Petruska, J., Janicek, P. (2006): Behaviour of the Wheel-Rail System Considering Shape Irregularities, Proc. of the 4th Dynamics of rigid and elastic bodies Conf., Usti n. L. (in Czech)

Johnson K. L. (1985): Contact Mechanics, Cambridge University Press

Kalker, J. J. (1990): Three Dimensional Elastic Bodies in Rolling Contact, Kluwer Academic Publishers.

Svigler J., Vimmr J. (2006): Contribution to Modelling of Wheel-Rail Contact, Proc. of the Engineering Mechanics 2006 Conf., Svratka (in Czech).